Analysis of Turbulent Flow Data Based on a Spectral Basis Representation

Prof. Dr. J. Garcke, Dr. R. Iza-Teran, C. Gscheidle
(Fraunhofer Center for Machine Learning and Fraunhofer SCAI, Germany);

L. Berger
(CFD Schuck Ingenieurgesellschaft mbH, Germany).

Abstract

Through the increase of computing power, Large Eddy Simulations (LES) have become an invaluable design tool for industrial applications. However, the increasing amount of data that is generated in each simulation imposes new requirements on data analysis and compression. Two shortcomings of classical approaches are addressed in this study. First, due to storage limitations, only a limited set of quantities can be extracted from the simulation, but needs to be selected in advance. This requires a-prior knowledge about the flow structure and an experienced user. Second, classical post-processing starts after the simulation is completed. Nevertheless, many effects occur at an early stage of the simulation and can give useful insights into trends. Data I/O and computing time can be reduced, if they are monitored carefully.

To address both issues, we apply a spectral basis approach for nonlinear dimensionality reduction to turbulent flow data. The spectral basis is derived from the eigenvectors of the Laplace-Beltrami (LB) operator which are optimal for representing smooth functions on a surface. The solution is projected to the LB basis to achieve a compact representation of the flow with a spectral separation. We demonstrate our approach on the LES of the turbulent flow through a HVAC duct that was studied intensively in the past, e.g. by *Jäger, A. et al., 2008*. Results are compared to a PCA analysis based on an extensive mesh study regarding their compactness and ability to identify large-scale and dominant flow features at an earlier state during the simulation.

1. Introduction

Through the increase of computing power, Large Eddy Simulations (LES) have become an invaluable design tool for industrial applications. Compared to Reynolds-Averaged approaches, LES provide more detailed insights into transient and turbulent effects over several length-scales. However, the large amount of data that is generated during the simulation requires new methods for data analysis and compression.

Two major shortcomings of classical approaches are addressed in this study. First, due to storage limitations, the entire flow data of LES can usually not be retained for all time steps and grid points. Therefore, only a limited set of quantities which are defined a priori of the simulation will be extracted during run-time. This requires an understanding of the physical effects of the flow before the simulation is set up and complicates the investigation of phenomenon that arise unexpectedly during the simulation. Second, classical post-processing starts after the simulation is completed. But fortunately, many effects already occur at an early stage during the simulation and can give useful insights into trends, e.g. grid dependency of the results. Data I/O and computing time can be saved, if they are monitored carefully.

In this paper, we apply two different dimensionality reduction techniques to the LES of the turbulent flow through a HVAC duct. As a practical relevant test-case from the automotive industry, the HVAC duct was studied intensively in the past (*Jäger, A. et al., 2008, Wang, C., 2013*) and offers several demanding flow features, notably pressure driven flow separation and flow around an obstacle. To start, we perform a Principal Component Analysis (PCA) which is successfully used for linear dimension reduction of a variety of types of data. Applied to flow data, *Frederich, O. and Luchtenburg, D., 2011* have shown the ability of PCA to extract dominant coherent structures from turbulence. These can then be used to investigate and characterize flows by different large-scale physical effects, such as vortex shedding or separation. However, in general, PCA are not able to pick up the spectral properties of turbulence and thus lacks the ability to clearly separate physical effects by their frequency or wave number. Besides, the principal axes only account for those statistical effects that they were trained on. They can become unstable in case of strong derivation or new features. To address both issues, we can construct a spectral basis that respects the geometrical boundaries of the test-case, is compact and independent of the flow solution. For car-crash simulations, a basis derived from the eigenvectors of the Laplace-Beltrami (LB) operator of a surface has successfully extracted spectral geometric modes that describe mechanical deformations (*Iza-Teran, R., 2017, Iza-Teran, R. and Garcke, J., 2019*). Here, we introduce an extension of the approach for the case of turbulence. In this case, the solution is projected to the LB basis to achieve a compact representation of the flow with a spectral separation. We compare both methods, using an extensive mesh study, regarding their compactness and ability to identify large-scale and dominant flow features at an early state of the simulation.

While we can demonstrate the potential of our LB based approach, further research will be necessary to develop a more compact basis that can resolve physical effects with high fidelity. For example, an improved statistical modeling of small-scale turbulent structures promises additional ways to identify flow features for analysis and classification purposes.

2. Laplace-Beltrami Operator for Nonlinear Dimensional Reduction

As used in *Iza-Teran, R., 2017* and *Iza-Teran, R. and Garcke, J., 2019* the Laplace-Beltrami operator is computed on a surface mesh embedded in three dimensional space. This operator is actually a Laplace operator, the difference is, that it is evaluated on the surface which is represented in three dimensional space.

The numerical evaluation of the LB operator requires the use of a metric that measures the distance along the surface. This distance is called geodesic distance and it is computed based on the shortest path algorithm for triangular surface meshes as described in *Mitchell, J. S. B. et.al 1987*. The approach in *Iza-Teran, R., 2017* and *Iza-Teran, R. and Garcke, J., 2019* was shown to provide a compact representation for functions defined on the mesh, for example the deformations. In general, for functions defined on a surface, it has been shown *Aflalo, Y. et.al., 2015* that the eigenfunctions of the Laplace-Beltrami operator are optimal for representing smooth functions. Let S be a given Riemannian manifold (e.g. a surface) with a metric g_{ij} and an induced Laplace-Beltrami operator, Δ_g, with associated spectral basis φ_i (the eigenfunctions), where $\Delta_g \varphi_i = \lambda \varphi_i$ (the eigenvalue problem). The representation error for any function $f \to \mathbb{R}$ is shown in *Aflalo, Y and Kimmel, R. 2013* to be given by,

$$\|\mathrm{r}_n\|_2^2 \equiv \left\| f - \sum_{i=1}^{n} \langle f, \varphi_i \rangle \varphi_i \right\|_2^2 \leq \frac{\left\| \nabla_g f \right\|_2^2}{\lambda_{n+1}}.$$

The optimality has been shown with the following result from *Aflalo, Y. et.al., 2015*.

Theorem 1. Let $0 \leq \alpha < 1$. There is no integer n and no sequence $\{\varphi_i\}_{i=1}^{n}$ of linearly independent functions in L^2 such that

$$\left\| f - \sum_{i=1}^{n} \langle f, \psi_i \rangle \psi_i \right\|_2^2 \leq \frac{\alpha \left\| \nabla_g f \right\|_2^2}{\lambda_{n+1}} \quad \forall f.$$

This means one can expect, depending on the degree of smoothness of the functions on the surface, to achieve a good representation using few components in the summation. Dimensionality reduction is then achievable using only few coefficients obtained through the scalar product $\langle f, \varphi_i \rangle$ (the spectral coefficients). We notice the analogy to the Fourier decomposition, where for smooth periodic functions the representation is also optimal and very compact. Data analysis can then be performed by using only those coefficients.

Flow data is three dimensional, but one can consider sections of the domain, for example the mid plane section or the duct walls. This gives as a result a geometrical surface. The proposed procedure of deriving a reduced representation of the flow data consists of two major steps:

1) *Evaluate the discrete Laplace Beltrami operator on each respective geometric surface and calculate the eigenvalue and eigenvectors.*

To reduce storage space, only the first ten percent of eigenvectors with the largest eigenvalues are determined. They form a subspace consisting of the spectral components with the largest spatial wavelengths. It is worth noting that the resulting basis solely depends on the geometry of the respective duct part and is independent of the flow solution. This computation is performed only once per geometry part, before the actual numerical simulation.

2) *Project all flow variables for each time step and part separately on the respective spectral basis*.

If the flow variables are vectors, each component, such as *Ux, Uy, Uz*, is treated independently. This results in one coefficient per basis vector, flow variable component, time step and geometry part. Considering the independence of the basis from the solution, the coefficients are particular suitable for a comparative analysis of large numbers of different simulations.

In a practical workflow the spectral basis has to be computed only once for each geometry part. This is done prior to the first transient simulation. During the run time of the simulations, the solution of one time step can be transformed to the new representation as soon as it is available. There is no need to store all transient flow data in order to perform an analysis afterwards and only the coefficients for the reduced basis are kept during run time. Besides, the projection onto the new basis can easily be done on subareas of the geometry, e.g. the meshes that result from the parallel execution of the core solver on different processes. In addition, it is possible to do this directly in memory which will reduce IO–operations considerably.

In Figure 1 an example vector of the spectral LB basis in the mid plane of the duct, parallel to the main flow direction, is shown. The spectral character of the basis can be observed by a sinus like spatial distribution. Besides, an influence of the geometric boundaries of the flap on the shape of the eigenvector in the center region can clearly be identified.

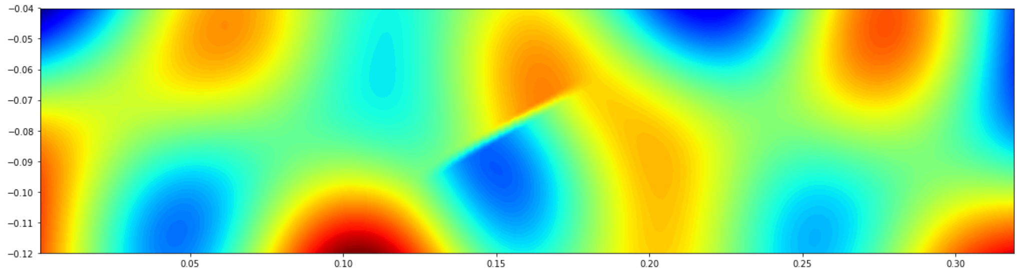

Figure 1: 18th eigenvector of the LB operator on the mid plane geometry of the duct

3. HVAC Test-Case and Numerical Setup

The turbulent channel flow through a HVAC duct was chosen as a suitable test case. It provides both, an industrial relevant application and complex flow features that allow the demonstration of advanced data analysis. The geometry is set up according to the description in *Jäger, A. et al., 2008* to allow a comparison with their experimental and numerical studies. It consists of a duct with a rectangular cross section and a bend of 90 degrees. In the lower part of the duct, a flap is placed with an angle of 30 degrees towards the wall. Inside the bend and behind the flap, a flow separation is observed. The resulting turbulent flow regions show an unsteady behaviour over several length scales of wave numbers and frequencies. The influence of four meshing parameters on these flow regions are investigated in this study.

In *Jäger, A. et al., 2008* this case was used to investigate aeroacoustic noise generation around the flap based on numerical and experimental results. Unsteady wall pressure fluctuations were measured at 7 positions within the HVAC duct by means of wall flush mounted 1⁄4 inch microphones (Figure 2) in the symmetry plane of the duct. The *Sound Pressure Level* (SPL) at these points is achieved by means of a *Fast Fourier Transformation* (FFT). In this study, the SPL are used for an initial validation of the numerical set up against the experiment. Most important features in the SPL are a characteristic peak at around 80Hz, as well as the decay of the spectrum for higher frequencies. For the FFT analysis, the parameters are set according to Jäger, A. et al., 2008 with a DFT length of 512 and 50% overlap for a frequency resolution of 4 Hz.

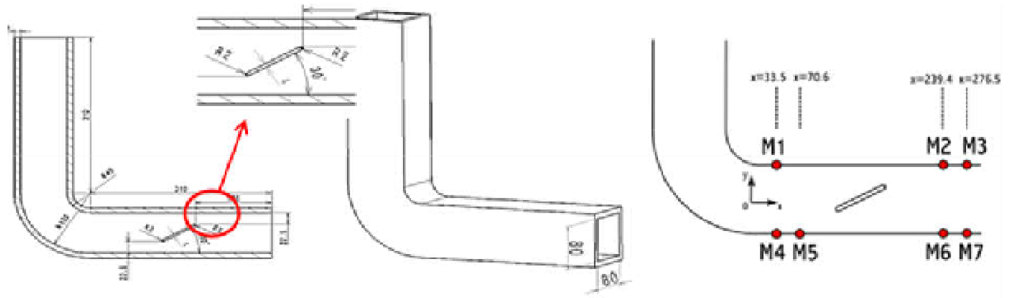

Figure 2: Geometric dimensions and sensor position of the HVAC duct (Jäger, A. et al., 2008)

To provide the necessary temporal and spatial resolution, *Detached Eddy Simulations* are performed with OpenFOAM version 2.4. The numerical set up is similar to the one described in *Wang, C., 2013*, although, in our study, a wall-function formulation is used to resolve the viscid sub layer at the wall boundaries. By this means, computing time will be saved in trade for a lower accuracy of the results. This can be justified by the preliminary focus of this study on data analytics rather than the investigation of the flow physics. The boundary conditions are set according to *Jäger, A. et al., 2008* with a vertical inlet velocity of 7.5 m/s. At the duct outlet, a large region of a coarse mesh layers are added to damp oscillations that can be reflected at the outlet boundaries. To ensure a fully developed turbulent flow in the area of the bent duct and the flap, a startup duct with 3 m length was attached to the inlet.

Mesh study and input parameter

Considering the usual workflow of setting up CFD simulations, mesh generation is the most time-consuming part for the engineer. On the one hand, the mesh quality and resolution need to be high enough to provide accurate results and enable confidence in the results. At the same time, a finer mesh resolution causes higher computing costs and thus the mesh should be kept as coarse as possible. One way to realize this is to refine only areas that contain large gradients of the flow solution or are of the highest interest for the evaluation. Nevertheless, these criteria are based on a-priori knowledge about the flow solution which require an experienced user. Similar issues arise from the numerical settings of the computational solver which can have a strong influence on the solution.

In this study, we want to create an automatic approach of identifying differences in the flow solution depending on global and local mesh properties and boundary condition. Thus, we define three mesh regions that are meshed independently with different resolutions. Additionally, we investigate the influence of a slipping boundary condition in the inlet duct compared to a wall function formulation. The mesh regions are marked in Figure 3. “Duct” refers to the area around the flap from x=0.6 to x=0.32, whereas the second region (“round”) includes the bent part of the duct. The mesh cell sizes in both regions are varied independently between 0.7 mm and 2.8 mm. The third region (“flap”) refers to the area closely around the flap. It has to be noted that the size of this region depends on its resolution. This is because the applied mesh generator, *SnappyHexMesh*, tries to provide a smooth transition between changing mesh resolutions and needs more space for larger differences.

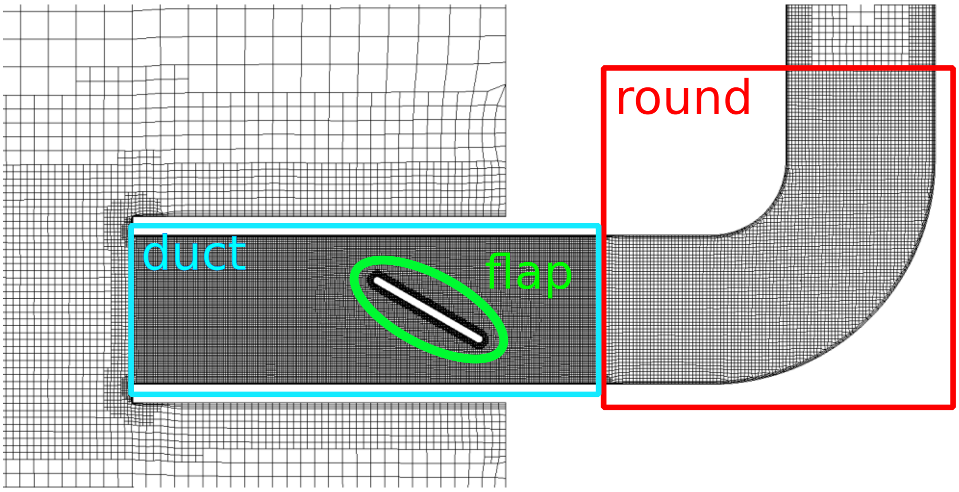

Figure 3: Refinement regions for the mesh study

While setting up the simulation, it was noticed that a slipping boundary at the inlet duct will prevent the channel flow to become completely turbulent before reaching the bend. Therefore, a longer inlet duct was created and wall friction was added, later called *Configuration I*. However, these first “wrong” results contain very useful knowledge for the mesh creation process and will thus be included in the analysis later on (*Configuration II*).

Table 1 summarizes the simulation cases and their mesh variations during the mesh study. Altogether 12 simulations are performed. The discretization scheme, solver settings, time step width Δt = 2E-5 and overall time steps N = 60,000 are held constant for all simulations.

Case	**Grid points** [mio]	**Config.** (I/II)	$\mathbf{\Delta h_{round}}$ [mm]	$\mathbf{\Delta h_{duct}}$ [mm]	$\mathbf{\Delta h_{flap}}$ [mm]
1	1.84	I	8	4	1
2	1.68	I	4	2	2
3	1.89	I	4	2	1
4	2.67	I	4	2	0.5
5	3.92	I	2	1	1

6	1.63	I	8	4	2
7	2.73	I	2	2	0.5
8	4.67	I	2	1	0.5
101	1.81	II	8	4	1
102	1.65	II	4	2	2
103	1.86	II	4	2	1
104	2.64	II	4	2	0.5

Table 1: Grid points and cell sizes for all cases of the mesh study

Automatic workflow and data extraction

The simulation workflow is sketched in Figure 4. Each parametric case includes an automatic mesh generation according to the input meshing parameters, calculation of an initial steady-state solution, and a transient *pisoFoam* run.

For data extraction, the built-in functionalities of OpenFOAM are used to define point cloud locations at which the static pressure values are recorded. For a simple comparison of different simulations, the point locations are kept constant. The interpolation of the flow solution at these positions is performed by OpenFOAM internally before the data is stored. The mesh resolution of the point cloud is set to match approximately the resolution of the finest computational mesh, in order to capture all spatial structures.

Three surfaces are defined to capture the flow at all regions of interest, including the bend, mid plane, and upper duct wall. Considering the temporal resolution that is needed for physical investigations of the aeroacoustics in the duct, the sampling frequency for data extraction is set to 5kHz. A simple low-pass filter is realized by extracting one snapshot every 10 numerical time steps that is time-averaged over the last 10 samples. This procedure will smooth out small temporal features and allows an accurate frequency resolution up to around 1kHz.

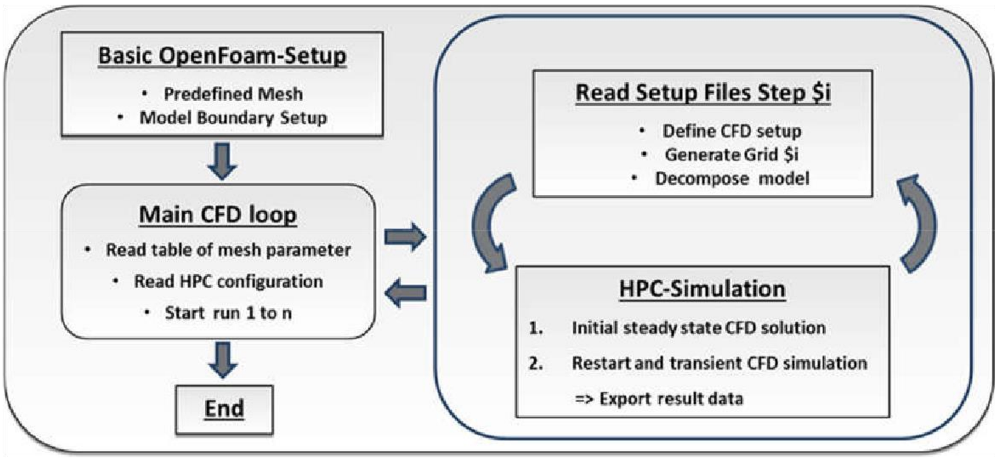

Figure 4: Automatic simulation workflow with OpenFOAM

4. Results

In this section, we present selected results from the mesh study. To provide a first validation of the numerical setup, we compare the pressure spectra at wall position 2 – as defined in Figure 2 – to the results from *Jäger, A. et al., 2008*. Second, the time dependent spectral coefficients at the outer duct of the bend are investigated for a bundle of ten simulations with respect to a change in the boundary condition of the underlying simulations. This is carried out for both the PCA and the LB-basis with a focus on their capabilities to identify a flow separation in some of the simulation after few time steps. Next, we want to assess the compactness of the PCA and LB basis, e.g. when used for compression of turbulent flow data. Pressure spectra at wall position 4 will be reconstructed from the respective spectral coefficients using only 2% of the components.

As mentioned before, the presented results are selected to demonstrate the principal characteristics and the potential of the proposed method for data analysis. In most cases, we concentrate on a few simulations and local flow behavior only. In order to perform a comprehensive mesh optimization, a global comparison of the results, at least including all regions and quantities of interest, is necessary. This could be based on the spectral coefficients or derived features and will be investigated in future research activities.

Wall Pressure Fluctuation at single positions

Prior to the investigation of advanced features, we want to build confidence in the numerical setup by investigating common flow properties. Thus, the sound pressure levels (SPL) at wall position 2, for two flow configurations, *Case 3* and *Case 103*, are plotted in Figure 5. Both consist of the same grid resolution in the duct, bend, and around the flap. However, the inlet duct in *Case 3* was extended from 1,5m to 3m to let the channel flow become fully turbulent before entering the bend. The experimental results from *Jäger, A. et al., 2008* are added for validation.

At wall position 2, the peak frequencies of the spectra agree well with the experimental results. Small differences in the amplitudes are in an expectable range. They can originate from uncertainties of the experimental setup or in the turbulence models as well as numerical errors. For higher frequencies, both simulations show more variance in the spectra then the experiment which can be explained by the smaller number of intervals that the spectrum is averaged over. For frequencies above 100 Hz, *Case 3* agrees well with the experimental results while *Case 103* induces much higher amplitudes. An explanation for this anomaly cannot be derived solely from the SPL spectra. Thus, further quantities need to be investigated. In a conventional engineering work flow, these are, for example, flow visualizations, boundary profiles, or wall shear stresses to find regions of separated flow or the like. In the following, we introduce a different approach by investigating the spectral coefficients of the LB and PCA-basis representation of the flow in the bend.

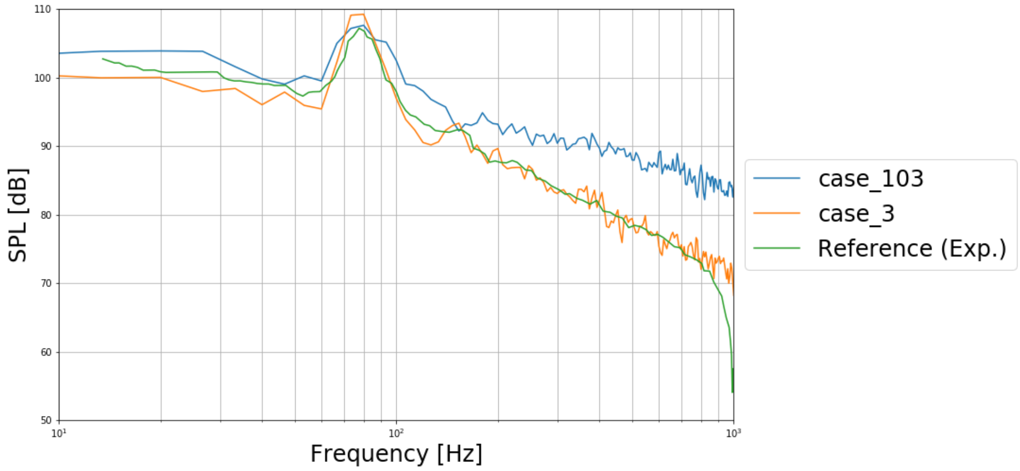

Figure 5: SPL at wall position 2 for Cases 3 and 103, experimental results from Jäger, A. et al., 2008

Spectral coefficients at outer wall of the bend

In the following, all 12 simulation runs with different meshing parameters are considered for a comparative analysis. As stated in Table 1, 0*Case 1 - 8* refer to configuration *Conf. I* with a long inlet duct, while for *Cases 101 - 104* a short inlet duct was used (*Conf. II*). The mesh resolution in the duct and bend are varied simultaneously for both configurations. For deriving a low dimensional representation of the flow data at the wall, two approaches are compared.

First, we construct the LB-basis on the outer bent duct geometry, as defined in section 3. Each static pressure solution snapshot is projected onto the newly derived basis. In Figure 6 a) the two spectral coefficients that exhibit the largest variance for the simulations with *Conf. II* are plotted for the first 0,2s (=500 time steps) of the simulation. Each point represents one snapshot for one transient simulation, starting from the initial steady state solutions that lie close together for all cases.

A clear separation of the results into two groups corresponding to *Conf. I* and *Conf. II* can be observed. The second configuration with a short inlet duct, shows considerably more variance over time. During the first 500 time steps, an oscillation with increasing amplitude develops from the initial solution for all simulations of *Conf. II*. This could result from a flow separation above the bend, when the distance from the duct inlet is not long enough for the channel flow to become fully turbulent. Hence, the flow is more prone to separation in this configuration. Once the separation occurs, the solver changes locally into a detached eddy mode and resolves the turbulent structures explicitly which ultimately results in a higher variance in the flow. The behavior can already be identified after a few time steps as follows from Figure 6 a). For *Conf. I,* the oscillation has a much smaller amplitude and frequency. Thus, the influence of the inlet duct length can clearly be identified. For example, this could be exploited for an optimization of the inlet duct without the need to run the simulation for the whole duration and can eventually save computing time.

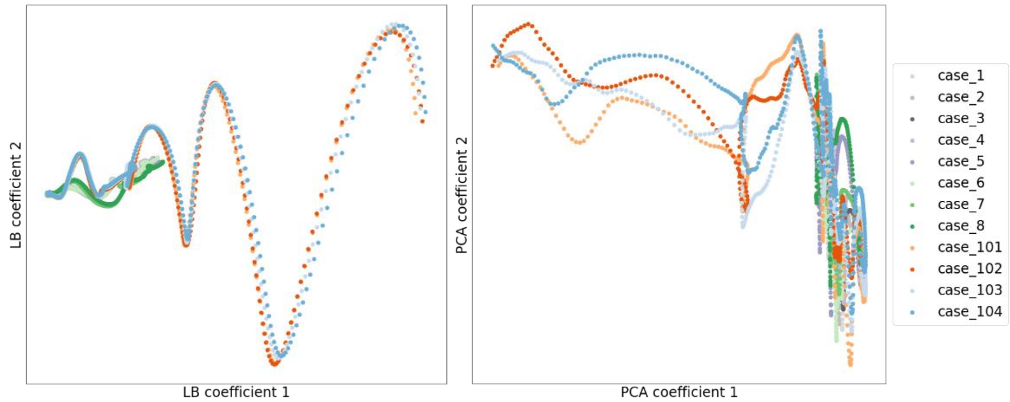

Figure 6: First two coefficients with largest variance for cases 1-8 and 101-104, from the projection of the static pressure solution at the bend's outer wall to a) the LB-basis and b) the PCA basis for the first 500 time steps

For the second approach, the spectral basis is construction by means of a principal component analysis (PCA). It is performed on a dataset of 600 Snapshots taken from *Case 3* with a constant temporal spacing spread over the entire simulation. The flow solutions of all time steps and simulations are projected onto the new basis, analogically to the workflow before with the LB-basis. Once again, the two coefficients with largest variance for *Conf. II* are evaluated in Figure 6 b). Although the two configurations can be identified, the distinction is not as clear as for the first approach. This can be explained by the way that the principal axes are constructed. By definition, the PCA finds those components that are the most compact representation of the underlying data, thus representing most variance. Nevertheless, in the training data taken from *Case 3*, no flow separation occurs in the bend region. Therefore, the newly appearing variations in *Conf. II* are not captured by a few principal components but rather spread over many components. In order to find a compact representation for the second configuration, we would need to recalculate the principal axis from the respective data. However, this would strongly change the shape of the axes and eventually make a comparative analysis unfeasible.

By an investigation of the LB - coefficients for *Cases 1-8* in Figure 7 for the first 200 time steps, an influence of the mesh resolution in the duct region can also be identified. The finer mesh for *Cases 5*, *7* and *8* leads to a clustering of the respective coefficients. This effect is small compared to the influence of the duct length and is not revealed by the PCA coefficients.

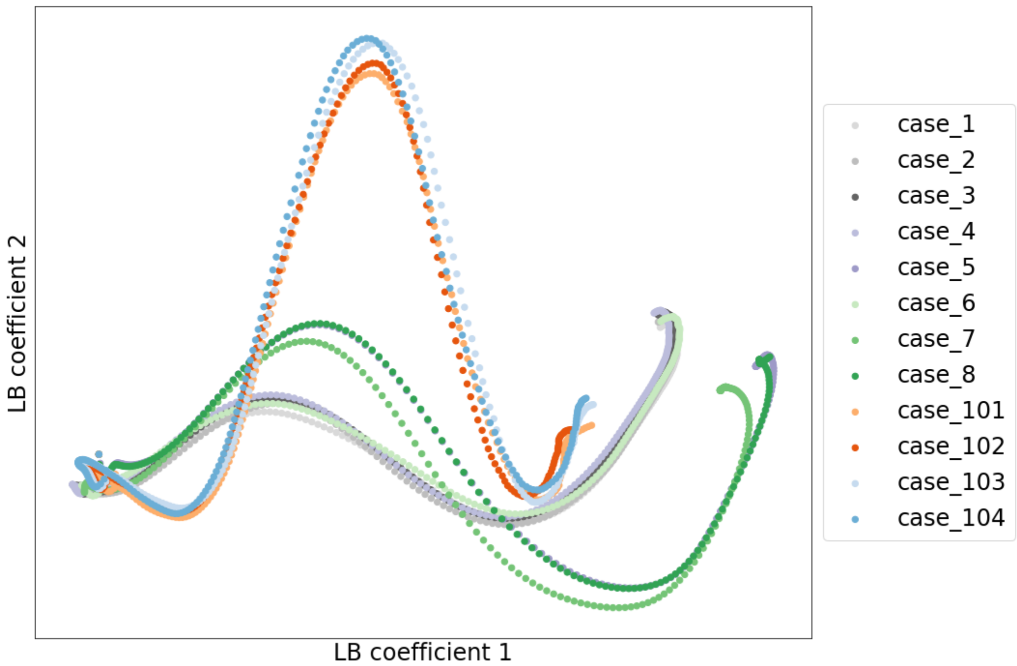

Figure 7: First 200 time steps for the same configurations as in Figure 6

Altogether, the LB basis provides a more precise clustering of the solutions depending on influential parameters, for the investigated example. Besides, the LB coefficients show smooth oscillations, while less clear structures are found in the PCA coefficients. Thus, the spectral characteristics of the LB eigenvectors seem to be more suitable to capture the temporal-spatial behavior of the investigated flow solutions. Particularly, its independence from the flow data prevents the spread of newly developing effects over several components as is the case for the PCA. This makes the LB operator to a promising technique for comparative data analysis tasks. More investigations are needed to assess its general capabilities of finding global and local differences in flow data for a variety of physical effects and flow behavior.

Compactness of LB basis and principal components

Next, we are interested in the accuracy of the reconstructed SPL spectra from a reduced number of components for each method. This addresses their ability to compress the flow data which can be regarded as a qualitative measurement for the compactness in a mathematical sense. While the PCA finds the most compact representation of a dataset for a given, reduced rank, it strongly depends on the data itself. Thus, we expect that the projection of a new dataset that differs from the original training data will be less compact. On the contrary, the LB basis is the most appropriate representation for smooth functions in a general sense, as described in Chapter 2, even though more compact bases can exist for a specific case.

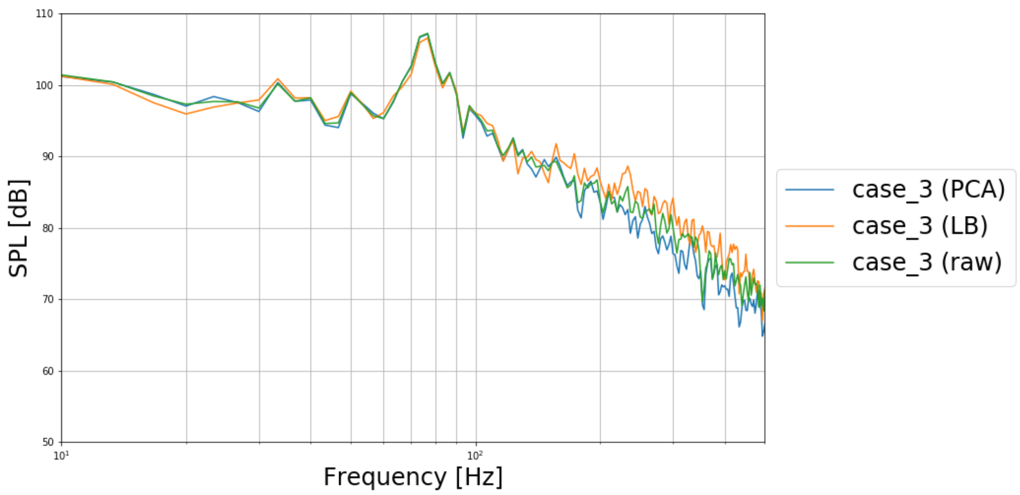

Figure 8: Reconstructed SPL spectrum for Case 3 from 2% of the eigenvectors of the LB and PCA basis

In Figure 8 and Figure 9 the reconstructed SPLs from the PCA and the LB basis formed on the mid plane geometry are shown alongside the original uncompressed data for *Case 3* and *Case 103*. The reconstruction was performed on the time depending pressure signal with 2% of the components of each basis. Afterwards, the SPL spectra are recomputed at wall position 4. This position is chosen because it provides large deviation between the training and test data and thus allows a more general evaluation of the compactness. As before, the PCA is trained on snapshots from *Case 3*.

For *Case 3*, differences between both signals are small. Altogether, the PCA provides a slightly better accuracy for most frequencies. This was expected because the PCA was trained on the same dataset as is used for testing. Nevertheless, the LB representation provides very accurate results up to around 100 Hz. For higher frequencies, larger differences to the uncompressed signal are observed while the general shape is still preserved. In general, this deviation for higher frequencies results from omitting higher eigenvectors that represent small spatial and temporal structures when reconstructing the flow solution. The error will increase for data that is less smooth and has more energy in higher frequencies, e.g. *Case 103*.

While the reduced PCA basis is able to rebuild the spectrum from its training data very well, the results for *Case 103* are considerably worse. Large errors occur for the whole spectrum with increasing magnitude for larger frequencies. As stated above, this can be related to the changed principal components of the new dataset due to newly occurring variations in *Case 103*. Thus the original PCA basis is less compact for the changed data. In contrast, the results from the LB basis reconstructions are similarly accurate as they were for *Case 3*. This underlines the higher general optimality of the LB basis compared to the PCA approach.

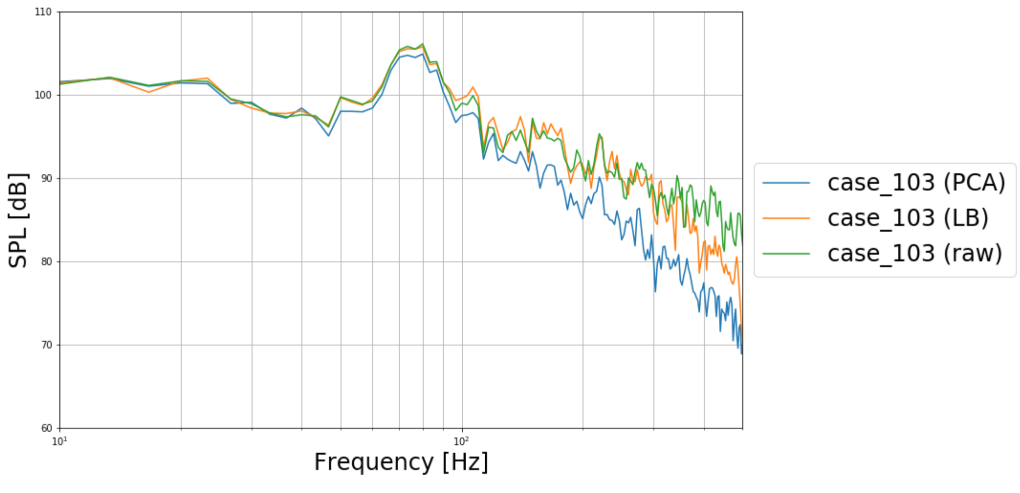

Figure 9: Reconstructed SPL spectrum for Case 103 from 2% of the eigenvectors of the LB and PCA basis

5. Conclusion

In this study, we proposed a new approach for the analysis of turbulent flow data. Thereby, the flow solutions are projected to a spectral basis derived from the Laplace-Beltrami operator on a geometric surface. The resulting coefficients are used for a comparative analysis of simulation bundles and compression of the flow fields. Results are compared to a PCA analysis with regard to the compactness of each representation and their capabilities to cluster the data by physical effects.

For the investigated example – the turbulent flow through a HVAC duct – the LB basis provides a more precise separation of the solutions depending on influential parameters. Besides, some of the LB coefficients show smooth oscillations while less clear structures are found in the PCA coefficients. This is in accordance with their behavior when used for data compression. While the PCA provides the most compact representation of a given data set, it can become much less compact when applied to new flow configurations. In contrary, the LB basis is more compact for a wider range of flows. In general, the spectral characteristics of the LB eigenvectors are more suitable to capture the temporal-spatial behavior of the investigated flow solutions. More investigations are needed to assess the general capabilities of the LB basis to identify global and local differences in flow data for a variety of physical effects and flow behavior including turbulent properties.

Beside a comparative analysis of simulation bundles, the observed results reveal interesting applications for data analytics based on the low dimensional representation of the flow data. If we consider only on a small number of components, it is practically feasible to store time dependent spectral coefficients for the whole simulation run. This way, we can reconstruct entire snapshots of the flow solution with a reasonable temporal and spatial accuracy. Eventually, the compressed data can be used to calculate derived features, such as POD or DMD modes, more efficiently and with less storage needed. A comprehensive parameter study with a global comparison of the results could be based on the spectral coefficients or derived global features. This will be carried out in future research activities.

Acknowledgement

This work was partially funded by the European Union's Horizon 2020 research and innovation programme within the project FORTISSIMO 2.

6. References

Jäger, A. et al. (2008), Numerical and Experimental Investigations of the Noise Generated by a Flap in a Simplified HVAC Duct, 14th AIAA/CEAS Aeroacoustics Conference (29th AIAA Aeroacoustics Conference), Vancouver, British Columbia Canada

Frederich, O. and Luchtenburg, D. M. (2011), MODAL ANALYSIS OF COMPLEX TURBULENT FLOW, Berlin University of Technology / Princeton University

Iza-Teran, R. (2017), Geometrical Methods for the Analysis of Simulation Bundles, PhD Thesis, University of Bonn

Iza-Teran, R. and Garcke, J. (2019), A geometrical method for low-dimensional representations of simulations. SIAM/ASA Journal on Uncertainty Quantification (accepted)

Mitchell, J. S. B. et.al (1987), The discrete geodesic problem. SIAM J. Comput., 16(4):647–668

Aflalo, Y. and Kimmel, R. (2013), Spectral multidimensional scaling, Proc. Natl. Acad. Sci. USA, 110, pp. 18052–18057.

Aflalo, Y. et.al. (2015), On the Optimality of Shape and Data Representation in the Spectral Domain, SIAM J. Imaging. Sciences, Vol. 8, No. 2, pp. 1141–1160.

Wang, C. (2013), Numerical Investigation of Flow Induced Noise in a Simplified HVAC Duct with OpenFOAM, KTH, Stockholm